DETERMINING ATMOSPHERIC COLUMN WATER VAPOUR IN THE 0.4 – 2.5μm SPECTRAL REGION

Andrew Rodger,* Mervyn. J. Lynch*

1 Introduction

To derive the surface spectral reflectance ρ(λ) from the radiance received at-sensor L(λ), correction is required for the effects of scattering and absorption. In the 400 to 2500 nm spectral region there are five major absorbing species, with the largest absorber being atmospheric water vapour (Green *et al*, 1991). The atmospheric water vapour is highly variable both spatially and temporally (Green, 1998) and has the effect of modifying the solar irradiance at the surface, which leads to the requirement to estimate the atmospheric column water vapour on a per pixel basis.

Current methods for water vapor estimation include the Continuum Interpolated Band Ratio (CIBR) (Bruegge *et al*, 1990) and the Narrow/Wide and Atmospheric Pre-Corrected Differential Absorption (APDA) (Borel *et al*, 1996; Schläpfer *et al*, 1996) technique. All of the methods make use of differential absorption techniques (Carrere *et al*. 1993), though a limiting factor is the way they are applied across a given atmospheric water vapour absorption feature; usually the 940 and 1130 nm absorption features. The accepted techniques use measurement channel/s and reference channel/s as described by Schläpfer (1996). One of the limiting factors of the traditional techniques is that only one estimate of column water vapor is gained for each water vapor absorption feature. This doesnt allow rejection schemes to be utilized or outliers to be readily identified. The use of linear interpolation across a given absorption feature to provide background surface reflectance slopes can also lead to problems when the surface under consideration has surface absorption features close to the atmospheric water vapour absorption features, this occurs with vegetated surfaces etc. Both of these problems may be overcome by modifying the form of the differential technique used, which in turn allows more of the 400 to 2500 nm spectral region to be utilised for the estimation of atmospheric column water vapour.

2 Radiative Transfer (RT) Theory

The spectral radiance at the sensor L(λ) may be expressed as the sum of the surface reflected radiance and the atmospheric path radiance $L_p(\lambda)$ (Liou, 1980). This is shown in equation (1).

$$L(\lambda) = \frac{\rho(\lambda)\mu_o E_o(\lambda)}{(1-\rho_b \bar{r})\pi}\gamma(\mu_o)\gamma(\mu) + L_p(\lambda), \quad (1)$$

where, the first term on the right hand side is the surface reflected radiance, ρ(λ) is the surface spectral reflectance at wavelength λ, μ_o is the solar zenith angle, μ is the sensor zenith angle, ρ_b is the background reflectance, $\bar{r}$ is the spherical albedo, $\gamma(\mu_o)$ is the downward transmittance, direct plus diffuse, at solar zenith angle μ_o and $\gamma(\mu)$ is the upward transmittance, direct plus diffuse, at zenith angle μ.

3 Power Series Form of the RT equation

If a single scattering regime is assumed, we have shown equation (1) may be recast, for a given surface spectral reflectance ρ(λ) in terms of the atmospheric column water vapor W and expressed as a power series of the following form (Rodger, 2000),

* Andrew Rodger <andrew_marie@bigfoot.com>, Mervyn. J. Lynch <tlynchmj@cc.curtin.edu.au>: Remote Sensing and Satellite Research Group. Curtin University of Technology, Perth, Western Australia

$$L(W,\lambda) = \sum_{k=0}^{n} a_k(\lambda) W^k \ , \tag{2}$$

where, $a_k(\lambda)$ is the k^{th} order coefficient at wavelength λ and W^k is the atmospheric column water vapor W raised to the k^{th} power. Equation (2) can be thought of as an approximating polynomial whose order is dependent on the spectral region under consideration. For example, in an atmospheric window region for a given wavelength λ and spectral surface reflectance ρ(λ), equation (2) reduces to a constant. As a water vapor absorption feature is approached the order required to represent the at-sensor radiance with equation (2) increases. In most cases the highest order required has been found to be a fourth order approximating polynomial. Further, if the radiance is represented as a function of atmospheric column water vapor W for *j* different values of water vapor, equation (2) becomes,

$$L_j(W,\lambda) = \sum_{k=0}^{n} a_{kj}(\lambda) W_j^{\ k} \ , \tag{3}$$

where j is used to differentiate between different atmospheric column water vapor amounts. Therefore, if a known surface reflectance $\rho(\lambda)$ is used in conjunction with known viewing and solar geometry, the radiance at a particular wavelength may be synthetically generated for a series of differing water vapor amounts (see figure 1). This is precisely what is applied to produce reference curves that allow the atmospheric column water vapor to be determined for a given L(λ).

4 Procedure Outline

To determine the water vapor W for an at-sensor radiance signal the following assumptions are made

- Single Scattering Regimes unless stated otherwise
- All reflectance calculations use atmospheric multiple scattering
- If aerosol is present an estimate of the visibility is known
- The navigation data and solar and viewing geometries for a given scene is known
- An accurate estimate of surface reflectance may be determined in spectral regions where the optical depth is small, (ie in the atmospheric window regions)

The following procedure is then implemented to estimate the atmospheric column water vapor W,

1. Estimate the surface spectral reflectance $\rho(\lambda)$ in the atmospheric window regions (Table 1) using equation (7). (see section **5**).
2. Forward model *j* synthetic at-sensor spectral signals, using a standard atmospheric type suitable to the time and region, and where each synthetic signal has a different amount of atmospheric column water vapor W and where each estimate uses the estimate of surface spectral reflectance $\rho(\lambda)$ that was determined in 1.
3. Scale the synthetic at-sensor spectral radiance and the measured at-sensor spectral radiance signal $L(\lambda)$ using equation , (10) for each signal. (see section **6**).
4. Establish spectrally dependent reference curves, using the synthetic signals from 3 using equation (15) (see section 7).
5. Estimate the atmospheric column water vapor, at reference wavelength λ, of the scaled measured at-sensor radiance using the reference curve that was established in 4.
6. Use the estimate of atmospheric column water vapor to repeat from steps 1 to 5 until an acceptable level of convergence has been reached[†].

5 Reflectance Determination in the Atmospheric Window Regions

To allow the accurate retrieval of atmospheric water vapor to proceed, estimates of the surface spectral reflectance in the atmospheric window regions is required. The purpose of this is to permit the generation of synthetic at-sensor scaled signals. The surface reflectance estimate is used in conjunction with an atmospheric

[†] When the procedure is repeated the estimate of atmospheric column water vapor that is determined in step 7 is used to forward model the synthetic signal that is used in step 1, and Table 1 has its limits changed to those given in Table 2.

modelling program, such as MODTRAN4.0 (Berk et al, 1999; Adler-Golden et al, 1999) to produce a series of synthetic at-sensor radiances that differ only in the amount of atmospheric water vapor. For the purpose of the following procedure, the atmospheric windows are defined in Table 1. It should be noted that the definition of the atmospheric windows in Table 1 are only used for an initial estimate of the atmospheric column water vapor W. After the initial estimate, the start and stop wavelengths/channels for each region are redefined and are shown in Table 2. The extended limits on the atmospheric window regions allow the retrieval of surface reflectance to take place within the wings of the atmospheric water vapor absorption features. This is possible because the first estimate of atmospheric column water vapor provides an improved estimate of the surface reflectance, and hence allows the estimation of surface reflectance to proceed into the wings.

It can be shown (Rodger, 2000) that a good estimate of surface reflectance in the atmospheric window regions can be found by performing the following procedure. Firstly, an estimate of the atmospheric path radiance $L_{mp}(\lambda)$ is removed from the at-sensor signal $L(\lambda)$ and from a synthetic signal $L_m(\lambda)$ that has a constant surface reflectance. Accordingly,

$$L(\lambda) - L_{mp}(\lambda) = \frac{\rho(\lambda)\mu_o E_o(\lambda)}{(1-\rho_b \bar{r})\pi}\gamma(\mu_o)\gamma(\mu)\,, \text{ and} \tag{4}$$

$$L_m(\lambda) - L_{mp}(\lambda) = \frac{\rho_m \mu_o E_o(\lambda)}{(1-\rho_{mb} \bar{r}_m)\pi}\gamma_m(\mu_o)\gamma_m(\mu)\,, \tag{5}$$

where, it is assumed that the solar zenith angle μ_o and the sensor zenith angle μ are known. Further, it is assumed that the spectral solar irradiance $E_o(\lambda)$ at wavelength λ is the same in the atmospheric modelling program of choice and the actual spectral solar irradiance observed on the day of acquisition. $L_{mp}(\lambda)$ is a synthetically generated estimate of the path radiance, and ρ_m is given as,

$$\rho_m = \text{constant}\,. \tag{6}$$

All other terms in equation (4) have been previously described. The terms in (5) have the subscript *m* added to signify a synthetically generated term or modelled quantity. As part of the scaling process equation (4) is divided by equation (5), and multiplied by equation (6), to produce equation (7). It is assumed that, since the regions of interest in atmospheric window regions, the optical depth and hence, gaseous absorption is minimal (Kaufman, 1989, 1984) and therefore the value of $\gamma(\mu_o)\gamma(\mu)/\gamma_m(\mu_o)\gamma_m(\mu)$ is close to unity. This can also be shown formally (Rodger, 2000). Further, the spherical albedo $\bar{r}$ multiplied by the background surface reflectance ρ_b is considered to be small (Kaufman, 1989) and as such is neglected. Therefore, the surface spectral reflectance $\rho(\lambda)$ in the atmospheric window regions is given as,

$$\rho(\lambda) = \rho_m \left(\frac{L(\lambda) - L_{mp}(\lambda)}{L_m(\lambda) - L_{mp}(\lambda)} \right). \tag{7}$$

The estimate of surface reflectance $\rho(\lambda)$ {see figure 2(a)} now is then used to write a spectral albedo file that is compatible with the atmospheric modelling program, MODTRAN4.0 in this case. In the spectral areas between the regions outlined in Table 1 and Table 2, MODTRAN4.0 will interpolate between the end values, so for example MODTRAN4.0 will interpolate between the 884nm reflectance value and the 1009nm reflectance value. Thus, an estimate of the reflectance in the absorption feature is gained. The estimate in the absorption feature is only deemed to be an approximation and is improved by implementing this procedure on an iterative basis. It is this estimate though that lends itself to accuracy when determining the column water vapor.

6 Transmittance Slope Ratio (TSR)

With techniques such as the CIBR and APDA, weighting is performed on the reference channels so as to provide a mean weighted radiance at the centre of an absorption feature. Rather than weight the reference channels it

is preferable to weight consecutive absorption features (ie the measurement channels). This can be thought of as a transmittance slope and is analogous with the reflectance slope that is used in other methods. The weighted mean radiance is given as,

$$\overline{L}_j(W,\lambda) = X_1(\lambda)L_{1j}(\lambda_1) + X_2(\lambda)L_{2j}(\lambda_2)\,, \tag{8}$$

where, $L_{1j}(\lambda_1)$ is the radiance at measurement channel 1 and wavelength λ_1 for the j^{th} value of atmospheric column water vapor, and $L_{2j}(\lambda_2)$ is the radiance at measurement channel 2 and wavelength λ_2 for the j^{th} value of atmospheric column water vapor. The weighting factor $X_1(\lambda)$ and $X_2(\lambda)$ are given as,

$$X_1(\lambda) = \frac{\lambda_2 - \lambda_i}{\lambda_2 - \lambda_1} \qquad \text{and} \qquad X_2(\lambda) = \frac{\lambda_i - \lambda_1}{\lambda_2 - \lambda_1}\,, \tag{9}$$

To produce a scaled radiance signal, or TSR value, equation , (10) is used {see figure 2(b)}, namely,

$$L_{s,j}(W,\lambda_i) = \frac{\overline{L_j}(W,\lambda_i)}{L_j(W,\lambda_i)}\ , \tag{10}$$

where, $L_{s,j}(W,\lambda_i)$ is the scaled radiance at wavelength λ_i and for atmospheric column water vapor value *j*.

7 Atmospheric Water Vapor as a Function of Radiance

To estimate the atmospheric column water vapor W for a given wavelength λ_i, the change in scaled radiance as a function of water vapor needs to be established. Writing the scaled at-sensor radiance of equation , (10) in a power series form yields the following,

$$L_{s,j}(W,\lambda_i) = \frac{X_1(\lambda_i)\left(\sum_{k=0}^{\infty} a_{1,k}(\lambda_1)W^k\right) + X_2(\lambda_i)\left(\sum_{k=0}^{\infty} a_{2,k}(\lambda_1)W^k\right)}{\sum_{k=0}^{\infty} a_k(\lambda_i)W^k}, \tag{11}$$

where, the numerator represents an approximating polynomial of a power series, as does the denominator. The numerator in equation (11) can be recast as a single power series, and as such, (11) is reduced to single power series given by,

$$L_{s,j}(W,\lambda_i) = \sum_{k=0}^{\infty} c_k(\lambda_i)W^k\ , \tag{12}$$

where,

$$\sum_{k=0}^{\infty} c_k(\lambda_i)W^k = c_0 + c_1W + c_2W^2 + \ldots + c_kW^k + \ldots \tag{13}$$

To retrieve the unknown water vapor W, equation (13) must be solved. This is not necessarily an easy task when it is in the form shown. Therefore, equation (13) is used in a form that has the dependent and independent variables interchanged such that now,

$$W = f(L_s(\lambda_i))\,, \tag{14}$$

$$W = \sum_{k=0}^{\infty} d_k(\lambda_i)\left[L_s(\lambda_i)\right]^k = d_0 + d_1\left[L_s(\lambda_i)\right]^1 + d_2\left[L_s(\lambda_i)\right]^2 + \ldots + d_k\left[L_s(\lambda_i)\right]^k + \ldots \tag{15}$$

where, $L_s(\lambda_i)$ is the TSR value for an unknown water vapor W. The coefficients of equation (15) are found from a least squares fit to synthetically generated TSR values of differing atmospheric column water vapor {see figure 2(c)}. The minimum order required for the approximating polynomial of equation (15) may also be found from the least squares fit, to date a third order has been found to be sufficient.

8 **Measurement Channels**

Three spectral sections are defined for the determination of atmospheric column water vapor. Each section contains two measurement channels and a number of reference channels. Located between the measurement channels, for a given section, are the reference channels. Shown in Table 3 are the channels that are used with AVIRIS as measurement channels and shown in Table 4 are the channels for each section that are defined as reference channels. It can be seen that if all three sections are utilised for the estimation of atmospheric column water vapor a total of 6 measurement channels and 32 reference channels are available, with each reference channel providing an estimate of atmospheric column water vapor.

9 **Performance & Evaluation**

Figures 3 and 4 show the results of using the procedure outlined. It is seen that it is effective over a range of targets, such as water {figure 3(a) and figure 4(b)}, vegetation {figure 3(c)} and other targets for all three sections. All targets (all charts in figures 3 and 4) show good agreement between all sections in the determination of water vapor. Differences between sections for a given pixel are attributed to surface absorption features located in the water vapor absorption features. These are not surface features that are close to the water vapor feature, rather they are surface features that overlay the water vapor absorption features. The ability of the procedure to work across a larger part of the spectrum is advantageous for a number of reasons. Firstly, a greater range of reference channels is utilised and hence a greater number of water vapor estimates are made from any given pixel. Secondly, preliminary testing suggests that section three is less prone to the effects of atmospheric aerosol and hence allows an estimate of water vapor to be made even if the aerosol loading is not known. Thirdly, the larger spectral freedom allows, in some cases, absorption features that are present in the water vapor absorption features to be verified as was illustrated in figure 4a. While not discussed in this paper, some caution should be observed when using sections two and three due to broad surface absorption features. These involve the use of small linear extrapolations. It should be remembered that the inclusion of surface reflectance estimates from the window regions is one of the major factors governing the success of this scheme and helps to overcome some of the major obstacles encountered by other methods.

10 **Conclusion and Recommendations**

The effectiveness of the procedure for determining atmospheric column water vapor in the 0.4 –2.5μm spectral region has proven to be highly successful. The procedure has been evaluated over different spectral materials and to date has not shown any major failures. A limitation to date is that no ground truth have been available to validate the procedure, and as such, it is recommended that in future work ground truth spectra be acquired and tested in conjunction with this procedure for the purposes of evaluation. All results shown also include output reflectance spectra from the commercial correction package ACORN as a form of validation. The performance of the procedure over dark targets has proven highly successful and has yielded results that are consistent with the surrounding water vapor for a given scene. It is recommended that over dark targets that the procedure is run for one iteration only. This provides a good estimate of atmospheric column water vapor and prevents looping of the estimate due to the dark nature of the target. Tests carried out on synthetic data sets to evaluate the accuracy of the procedure have shown an accuracy of around 1-2%, in reality though this is expected to be higher due to incorrect modelling and other factors such as aerosol contamination and random instrument effects. It is expected that this procedure can be used in a Look Up Table (LUT) procedure. A comprehensive sensitivity analysis will also be carried out in the near future.

11 **Acknowledgments**

Many thanks to Dr Thomas Cudahy from CSIRO Exploration and Mining Division, Floreat Park, Perth Western Australia, for financial assistance for one of the authors (AR) to attend the 2001 AVIRIS workshop and for being a great sounding board for ideas. Thanks to Gail Anderson from NOAA for answering AR's endless questions about MODTRAN4.0, and many thanks to Robert. O. Green from the AVIRIS science team at NASA JPL for also answering the never-ending stream of questions concerning AVIRIS.

12 **References**

Adler-Golden, S.M., M.W. Matthew, L.S. Bernstein, R.Y. Levine, A. Berk, S.C. Richtsmeier, P.K. Acharya, G.P. Anderson, G. Felde, J. Gardner, M. Hoke, L.S. Jeong, B. Pukall, J. Mello, A. Ratkowski, H.-H. Burke, (1999), Atmospheric Correction For Short-Wave Spectral Imagery Based On MODTRAN4, Airborne Visible/Infrared Imaging Spectrometer (AVIRIS) 1999 Workshop Proceedings, Jet Propulsion Laboratory, Pasadena, CA

Berk, A., G.P. Anderson, L.S Bernstein, P.K. Acharya, H. Dothe, M.W. Matthew, S.M. Adler-Golden, J.H. Chetwynd, Jr., S.C Richtsmeier, B. Pukall, C.L. Allred, L.S. Jeong, M.L. Hoke, (1999), MODTRAN4 Radiative Transfer Modeling For Atmospheric Correction, Airborne Visible/Infrared Imaging Spectrometer (AVIRIS) 1999 Workshop Proceedings, Jet Propulsion Laboratory, Pasadena, CA

Borel, C.C., D. Schläpfer, (1996), Atmospheric Pre-Corrected Differential Absorption Techniques To Retrieve Columnar Water Vapor: Theory And Simulations, Airborne Visible/Infrared Imaging Spectrometer (AVIRIS) 1996 Workshop Proceedings, Jet Propulsion Laboratory, Pasadena, CA

Bruegge, C.J., J.E. Conel, J.S. Margolis, R.O. Green, G. Toon, V. Carrère, R.G. Holm, G. Hoover, (1990), 'In-Situ Atmospheric Water-Vapor Retrieval in Support of AVIRIS Validation', *Imaging Spectroscopy of the Terr. Environ, SPIE* **1298**, 150-163

Carrère, V., J.E. Conel, (1993), 'Recovery Of Atmospheric Water Vapor Total Column Abundance From Imaging Spectrometer Analysis And Application to Airborne Visible/Infrared Imaging Spectrometer (AVIRIS) Data', *Remote Sens. Environ*, **44**, 179-204

Green, R.O., J.E. Conel, J.S. Margolis, C.J. Bruegge, G.L. Hoover, (1991), An Inversion Algorithm for Retrieval of Atmospheric and Leaf Water Absorption From AVIRIS Radiance With Compensation for Atmospheric Scattering, Airborne Visible/Infrared Imaging Spectrometer (AVIRIS) 1991 Workshop Proceedings, Jet Propulsion Laboratory, Pasadena, CA

Green, R.O., (1998), Apparent Surface Reflectance of the DOE ARM SGP CART Central Site Derived from AVIRIS Spectral Images, Airborne Visible/Infrared Imaging Spectrometer (AVIRIS) 1998 Workshop Proceedings, Jet Propulsion Laboratory, Pasadena, CA

Kaufman, Y.J, (1984), 'Atmospheric Effects On Remote Sensing Of Surface Reflectance', *SPIE*, **475(6)**, 20-33

Kaufman, Y.J, (1989), *Theory and Applications of Optical Remote Sensing*, John Wiley and Sons, New York, chapter The Atmospheric Effect on Remote Sensing and Its Correction, 336-428

Liou, K., (1980), *An Introduction to Atmospheric Radiation*, Academic Press, Inc. New York, chapter Principle of Multiple Scattering in Plane-Parallel Atmospheres, 176-230

Rodger, A., (2000), Estimation of Atmospheric Column Water Vapor and Surface Reflectance Determination Using Remotely Sensed Hyperspectral Data, Report No: SPS 714/2000/AP97, School of Physical Sciences, Curtin University, Perth, Western Australia.

Schläpfer, D., C.C. Borel, J. Keller, K.I. Itten, (1996), Atmospheric Pre-Corrected Differential Absorption Techniques To Retrieve Columnar Water Vapor: Application To AVIRIS 91/95 Data, Airborne

Visible/Infrared Imaging Spectrometer (AVIRIS) 1996 Workshop Proceedings, Jet Propulsion Laboratory, Pasadena, CA

13 **Tables and Figures**

Table 1: The defined atmospheric window regions that are used to determine surface reflectance in preperation for the estimation of atmospheric column water vapor.

Region	Start Wavelength (nm)	End Wavelength (nm)	Start AVIRIS Channel	End AVIRIS Channel
1	875	884	55	56
2	1009	1067	69	75
3	1230	1284	92	100
4	1543	1702	126	142
5	2078	2088	181	182

Table 2: The defined atmospheric window regions that are used to determine surface reflectance in preperation for the estimation of atmospheric column water vapor after an initial estimate has been made.

Region	Start Wavelength (nm)	End Wavelength (nm)	Start AVIRIS Channel	End AVIRIS Channel
1	875	913	55	59
2	961	1105	64	79
3	1163	1314	85	103
4	1463	1722	118	144
5	1978	2088	171	182

Table 3: Consecutive measurement channels used to define an section. An interval has the measurement channels at the start and end of each section and contains the reference channels within each section.

Section	M1 Wavelength (nm)	M2 Wavelength (nm)	Measurement Channel 1	Measurement Channel 2
1	942	1124	62	81
2	1124	1334	81	105
3	1443	1782	116	150

Table 4: The reference channels available for each section outlined in Table 3.

Section	Reference Channels (nm)	Reference Channels
1	980 – 1086	66 – 77
2	1201 – 1274	89 -99
3	1563 - 1642	128 - 136

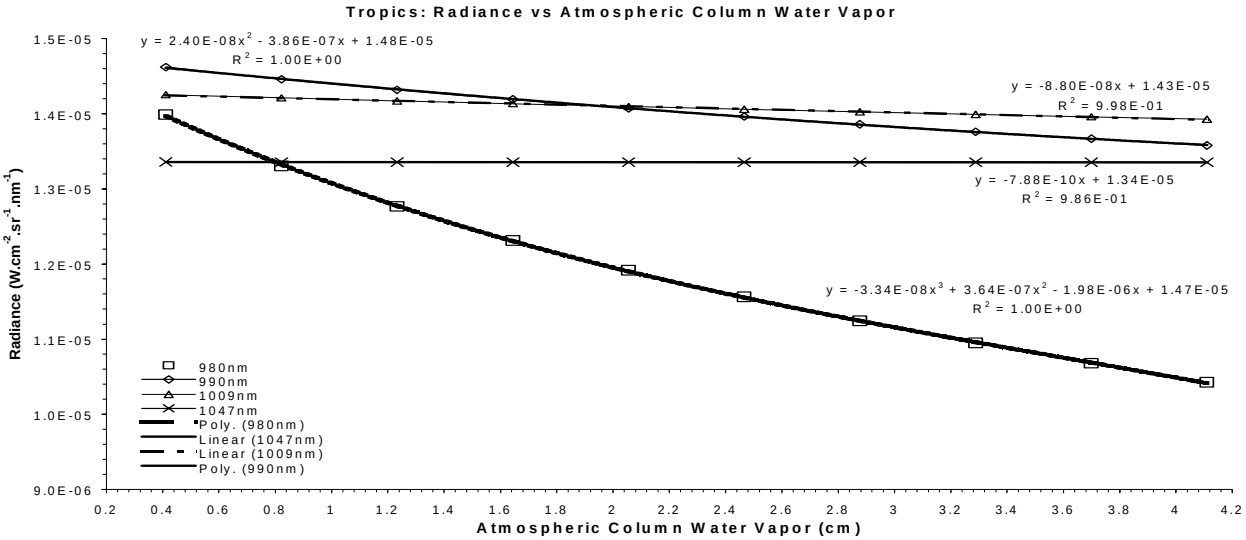

Figure 1: The radiance at-sensor as a function of atmospheric column water vapor and for a given surface spectral reflectance. Four different wavelengths are shown, they demonstrate that the radiance can be represented by an approximating polynomial. The order of which is dependent on the region under consideration. As the water vapor absorption feature (940nm) is approached the order of the polynomial is seen to increase.

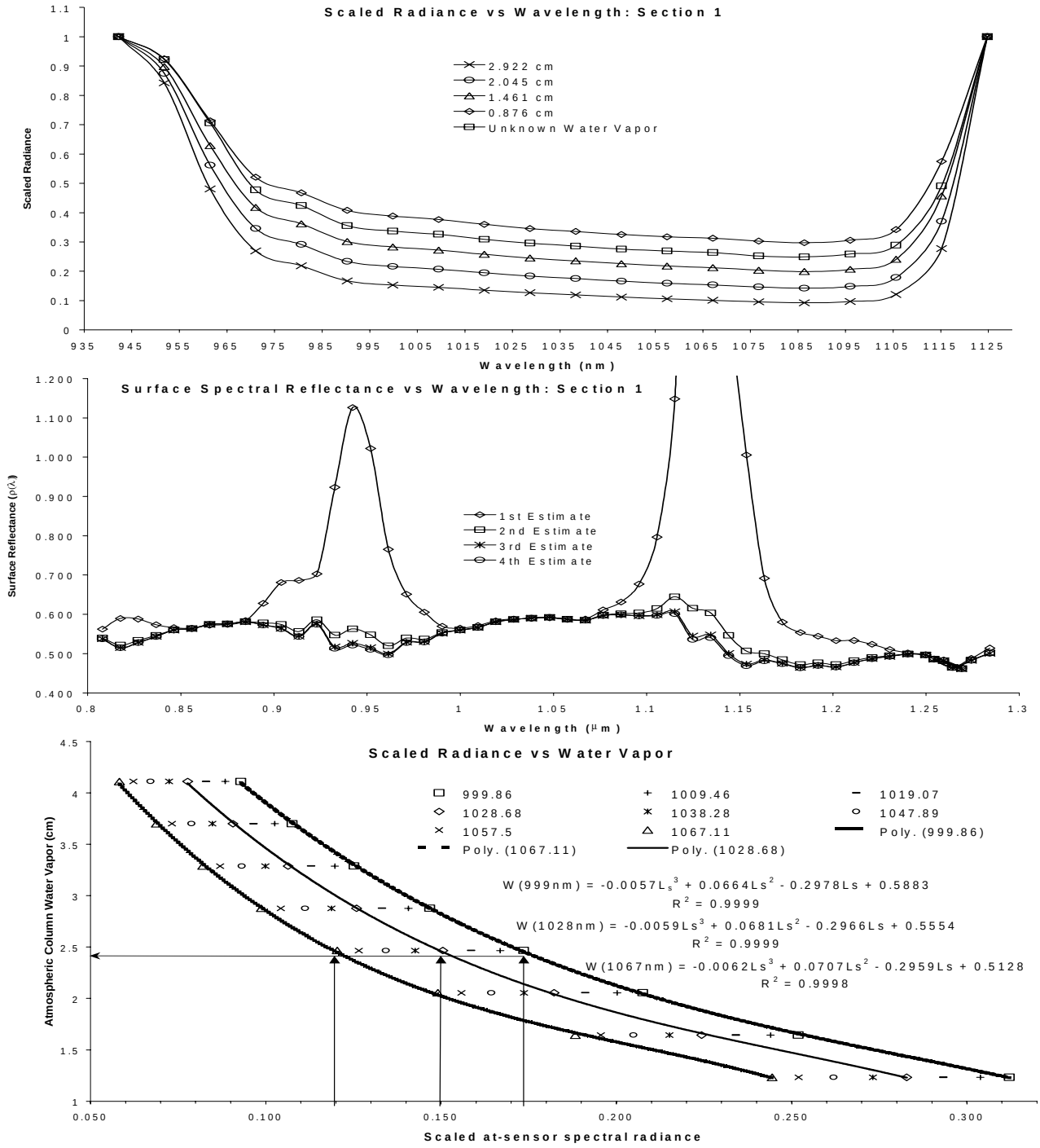

Figure 2: Top (a), Retrieval of surface reflectance with increasingly improved estimates of atmospheric water vapor. Only the wavelengths shown in Table 1 and 2 are used. When Table 2 is used the retrieval effectively occurs in the wings of the atmospheric water vapor absorption feature as well. **Middle (b)**, Scaled radiance as a function of wavelength. An estimate of surface reflectance has been made and used to produce synthetic at-sensor radiance with the different atmospheric column water vapor amounts shown. The at-sensor signal of unknown atmospheric column water vapor is seen to lie between 1.461 and 0.876 cm of water vapor. **Bottom (c)**: Reference curves used to estimate atmospheric water vapor of a pixel that has had the surface reflectance estimated in the atmospheric windows. The arrows indicate the direction of the estimate. A scaled at-sensor radiance (measured) value is determined for a given wavelength, which is related to an amount of atmospheric column water vapor.

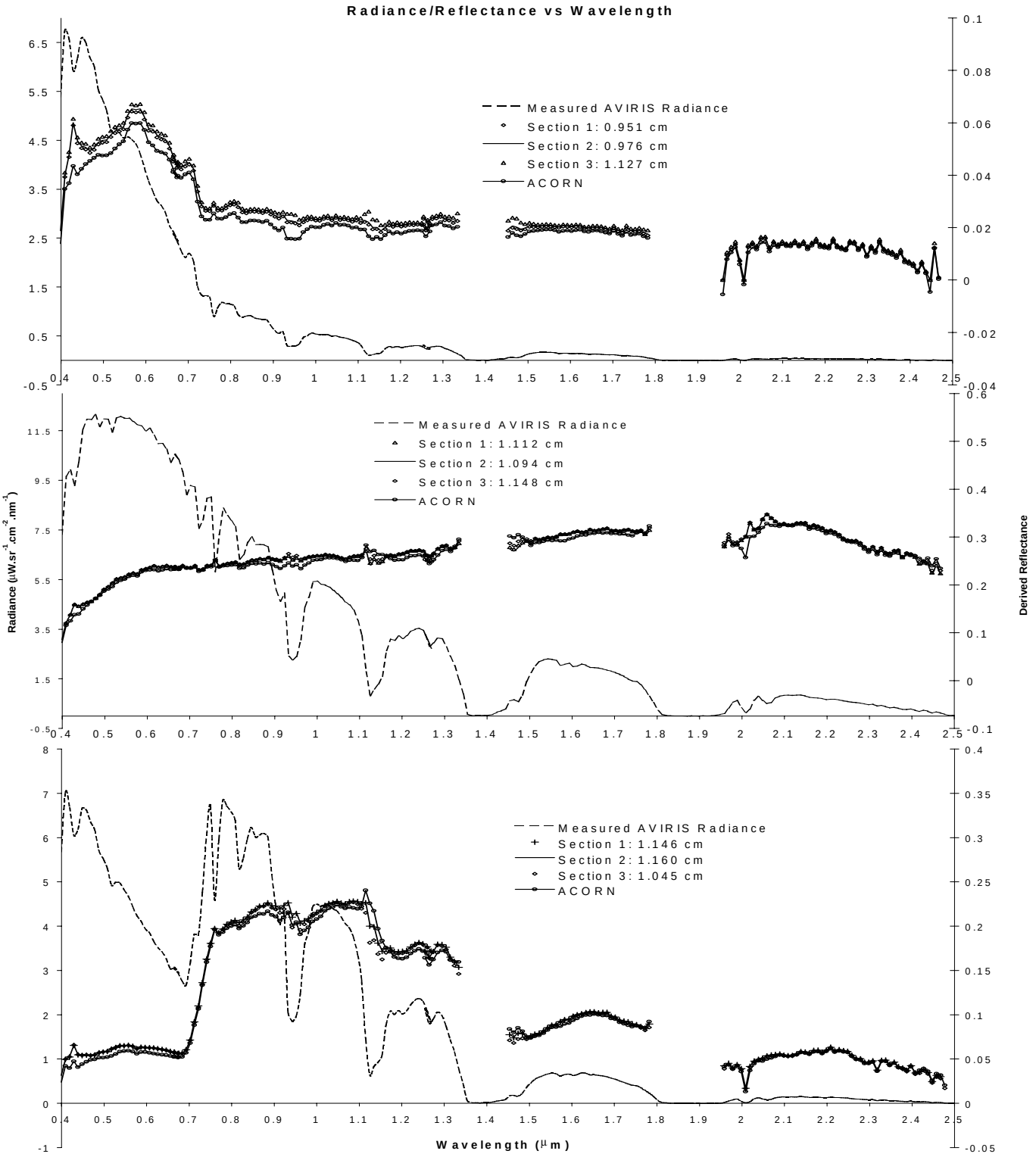

Figure 3: Moffett Field 1997. Derived surface reflectance for all 3 section. **Top (a)**, Pixel 188 line 93 scene3. Standing water target. **Middle (b)**, Pixel 503 line 165 scene3. Tarmac located at Moffett field airbase. **Bottom (c)**: Pixel 602 line 19 scene3. Vegetation target

All three figures (a), (b) and (c) show the amount of water vapor, in cm, derived for each section. The agreement, for atmospheric column water vapor, between the three different intervals is good except in the case of the standing water, where section 3 shows a higher water vapor value. The pixel in (c) is over shallow water and therefor the higher value in section 3 may indicate a surface absorption feature at 1.4 micron.

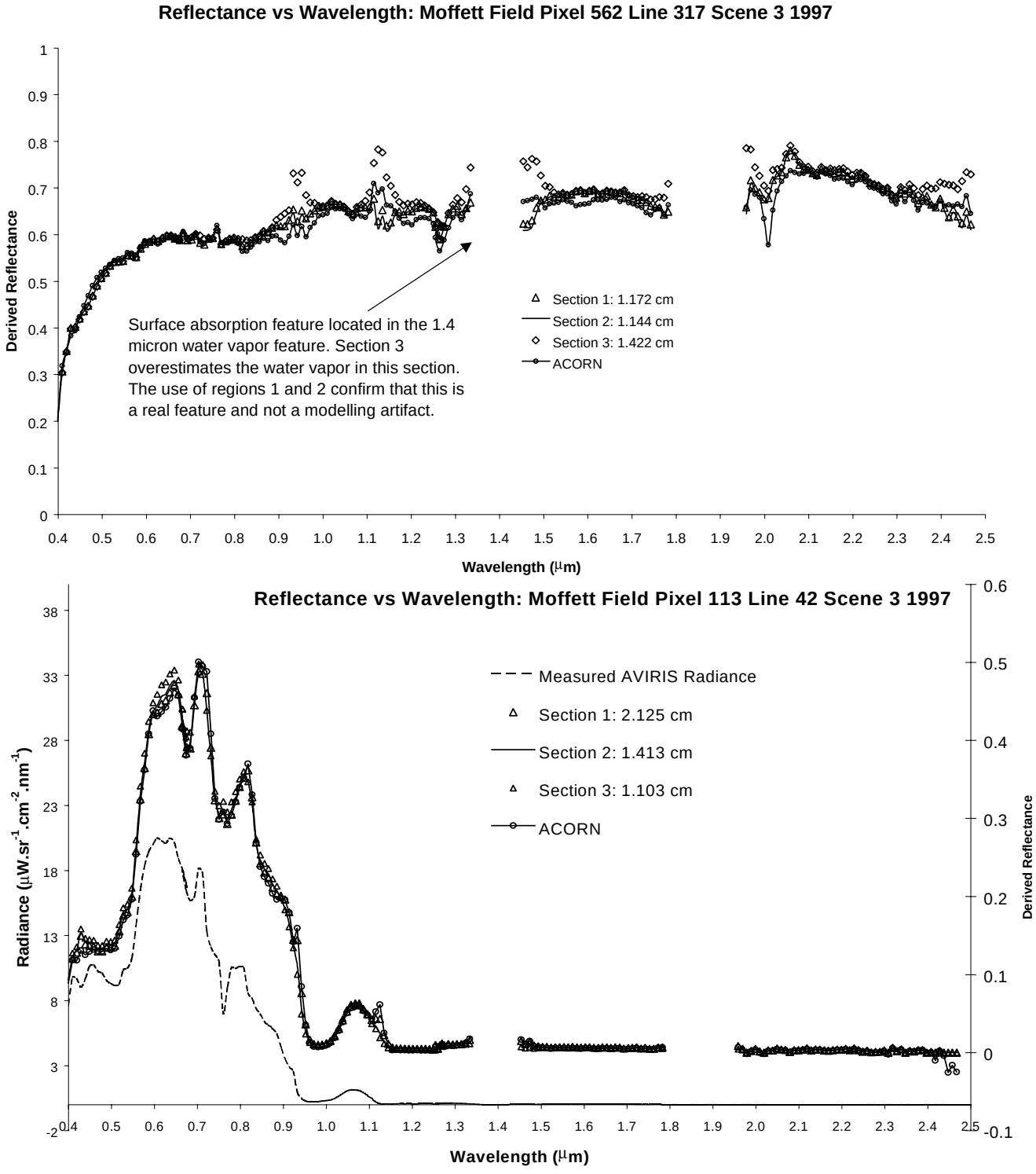

Figure 4: Moffett Field 1997. Derived surface reflectance for all 3 sections **Top (a)**, Roofing material. Note the agreement from sections 1 and 2 for atmospheric column water vapor, thus confirming a surface absorption feature located in the 1.4 micron water vapor absorption feature. The surface absorption feature causes section 3 to overestimate water vapor. **Bottom (b)**: Salt+standing water in the salt reservoirs at Moffett Field. Again a large surface absorption feature in the 0.94 micron region causes and overestimation of water vapor. This is confirmed with consistent results for sections 2 and 3. It should be remembered that each estimate from each section is an average of approximately 10 separate estimates of water vapor. A suitable rejection scheme would discount outlier results caused by deep surface absorption features locate din the water vapor absorption features.